Multimode fibre laser Doppler anemometer with directional discrimination and high spatial resolution for the investigation of turbulent boundary layers

by

Lars Büttner and Jürgen Czarske

Laser Zentrum Hannover, Group Laser Metrology
Hollerithallee 8; D-30419 Hannover; Germany

Internet: http://www.lzh.de, email: lb@lzh.de

ABSTRACT

The advantageous employment of multimode fibres for beam delivery in laser Doppler anemometers (LDA) is presented. Multimode fibres allow the transfer of significantly higher power into the LDA measurement volume and need lower alignment effort compared to the usually employed singlemode fibres. Powerful laser diodes can now be applied for LDA set-ups, enabling sensitive velocity measurements of fluid flows.
However, due to the obeserved signal degeneration caused by the speckle-effect, this technique could never become established. In this work the speckle pattern of the multimode beam is sufficiently suppressed by choosing high-aperture fibres with high intermodal dispersion and by the use of laser diode arrays with low coherence lengths, see figure (1).
It is demonstrated, that the length of the measurement volume is reduced to a few percent compared to the intersection volume length of the two laser beams because of the low spatial coherence of the multimode light. The long axis of the measurement volume is in this case aligned in the flow direction, whereas in conventional LDA´s employing single mode radiation it is perpendicular.
The uniformity of the fringe spacing is significantly improved. The variation of fringe spacing, pretending a non-existing degree of turbulence ("virtual turbulence"), is less than 0.1%.
The multimode-fibre LDA (MMF-LDA) combines the advantages of both a short measurement volume guaranteeing a high spatial resolution as well as low virtual turbulence in one device. It is therefore well suited for high accurate determination of velocity gradients in laminar or turbulent boundary layers.
A MMF-LDA with 80 µm measurement volume length, about 100 fringes and $5 \cdot 10^{-4}$ fringe spacing variation was used to perform fluid measurements in a wind tunnel. The remaining degree of turbulence of the wind tunnel was determined to 0.3%. Boundary layer measurements on a well-known laminar velocity profile, the Blasius boundary layer, were performed and the wall shear stress was determined. All results are in excellent agreement with the theory.

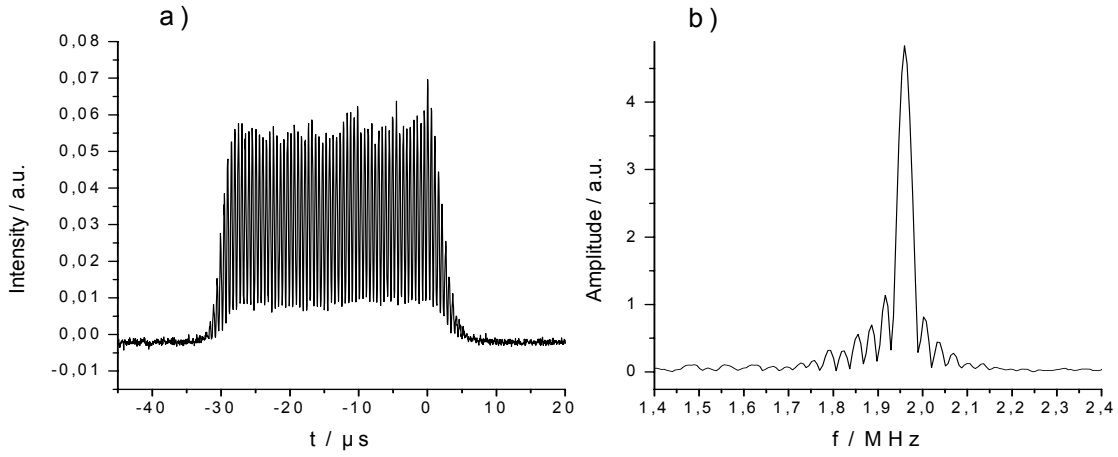

Figure 1: Burstsignal of a small water droplet passing through the measurement volume in the a) time domain and b) frequency domain. Speckles, appearing as non-periodic oscillations on the signal´s envelope, are sufficiently suppressed .

I. Introduction

The measurement of velocity gradients in fluid flows is of great interest in fluid mechanics. Detailed information about the velocity distribution is a prerequisite for the defined design of aerodynamic devices like aircraft wings, micro-nozzles, etc. Another typical application in tube flows is the measurement of velocity profiles, from which the flow rate can be evaluated exactly. In the field of medicine, special interest exists in the local resolution of velocity fields in veins or arteries.

In fact, the often applied and well-established laser-Doppler-anemometers (LDA) can be used for the resolution of velocity gradients only under certain conditions. The common LDA-technique is known as a quasi-point-like measurement technique. This means that the velocity information of the whole fluid field can not be registered simultaneously but only by local sectioning. For the measurement of the whole velocity, field mechanical scanning is afforded. The spatial resolution is determined by the finite size of the measurement volume. Since its length is usually about one millimetre, the resolution of velocity gradients is difficult. To overcome this drawback, the following two methods are conventionally used:

A) Spatial restriction through the receiving optics, i.e. reduction of the acceptance field of the detector
B) Spatial restriction through the sending optics, i.e. reduction of the length of the measurement volume

In method A), the restriction of the acceptance field of the detector is usually done by means of beam stops or confocal imaging. As a consequence, greater effort is required for the adjustment of the detection unit and the laser power is only partially used.
Also applied is method B), where one work shall be mentioned here exemplarily: In [1] the migration of platelets and red blood cells in highly diluted suspensions was studied. For this purpose an LDA-measurement volume with a lateral size of 5.7 µm and a length of 19 µm was provided and the velocity profile in a rectangular flow channel of 100 µm width was measured. Such a short measurement volume was obtained by a small focus, resulting in a working distance below 4 mm and a crossing half angle of 17.2°.

In general, strong focusing usually goes along with a short working distance. However, longer working distances are often required, but since the entrance window to a flow tube is of a finite size, the beam crossing angle is limited for a given working distance and the size of the measurement volume can not subside below a certain value. Furthermore it can be shown [2] that the variation of the fringe spacing increases inversely proportionally to the square of the beam waist diameter in the measurement volume. Since the longitudinal position of the passing particle in the measurement volume is usually not known, the spectral width of the Doppler line broadens, which can regarded as a virtual turbulence. Therefore, the design of an LDA-system is a compromise between high spatial resolution - given by the length of the measurement volume - and the accuracy of the velocity measurement, given by the variation of the fringe spacing. The presented principle of the multimode-fibre LDA reduces this complementarity, as shown later.

The advantages of fibre-optic transmission and receiving LDA-systems, like flexibility and immunity against electromagnetic disturbances, were early recognized [3]. In general, single-mode fibres are applied for beam delivery from the laser to an optical measuring head to preserve beam quality and spatial coherence properties. On the other hand, attempts with graded-index multimode fibres have been made to take advantage of the low incoupling efforts and higher transmittable powers [4,5]. But due to the observed degradation of the signal quality, up to now the employment of multimode fibres for beam delivery could never become established.

This work presents a multimode-fibre-LDA-system (MMF-LDA), which minimises the signal degradation caused by the speckle effect and allows the generation of short measurement volumes with low measurement errors. This can be achieved by the use of light emitted from a multimode fibre. The multimode fibre reduces the degree of spatial coherence, so that the length of the interference volume is reduced drastically. With this simple principle a better adaption to the measuring principle is attained, since measurement volumes can be generated with their long axis in the measurement direction and their short axis along the optical axis, whereas in LDA´s using singlemode-radiation it is vice versa, see fig. (7) in chapter III. Furthermore multimode fibres are suitable for delivering high power into the measurement volume. Due to their large core diameters the incoupling is on the one hand less sensitive and on the other hand much more efficient, so that low-cost and high-power light sources even with a poor beam quality can be employed for LDA measurements, e.g. Nd-YAG lasers and high-power diode lasers like diode arrays, broad-area diodes, etc.
Today high-power diode lasers are commercially available with output powers up to 6 kW [6]. Features like high electro-optical efficiency, compact designs and long lifetimes are obtained. At the moment, their main application field is laser material processing. However, since the range of application in this area is still widening, further developments towards higher power, better beam qualities and lower prices due to mass production can be expected. Today, 500 W laser diode power out of a 600 µm multimode fibre is commercially available [6], which demonstrates the potential for LDA systems arising from the employment of multimode fibres.

The aim of the present work is to qualify the employment of multimode fibres for beam delivery in LDA-systems. The article is structured as follows:
In chapter II those features of the LDA which are affected by the employment of multimode fibres are outlined and briefly explained. Chapters III contains a description of the experimental set-up as well as characterisation of the properties of the MMF-LDA. Chapter IV demonstrates, how the set-up can be extended to achieve directional discrimination by means of the two-wavelength homodyne-technique. In Chapter V results from Blasius boundary layer measurements are presented and compared with theory. Chapter VI summarises the results.

II. Effect of multimode laser beams on the laser-Doppler fringe system

In the following, the most common set-up principle of a laser-Doppler-anemometer, the differential Doppler technique, is considered.
The light emitted from a multimode fibre is a superposition of all guided modes. Such a multimode radiation outside the fibre can be characterised by the dimensionless beam quality factor or propagation factor M^2. It is equal to 1 for ideal Gaussian beams but greater than 1 for most real beams, especially transversal multimode-beams. The beam quality factor of the light emitted from a multimode fibre with a core diameter D and numerical aperture A_N can be approximated by [7]

$$M^2 \approx \frac{\pi \cdot D \cdot A_N}{2 \cdot \lambda} \tag{1}$$

It is important to note that this standard value is a valid estimation of the output beam quality only in case of equilibrium mode distribution. It can be used to estimate the beam quality of the emitted radiation. Experimentally, the intensity profile and the far-field divergence angle θ and therefore the M^2-value are strongly affected by the incoupling conditions. On the other hand it is well known that bending of the fibre leads to power exchange between different modes [7,8,9], so that a mode distribution just like that of an unbent but very long fibre is achieved. Such a mode scrambling induces on the one hand a small power loss, but on the other hand an output intensity profile, which is stable and almost independent of the launching conditions.

The propagation of light in different modes within a multimode-fibre is a statistical process, so that correlation between different modes gets lost. Since the emitted light is a superposition of all guided modes, the degree of spatial coherence - characterised by the coherence distance, defined below - is reduced.

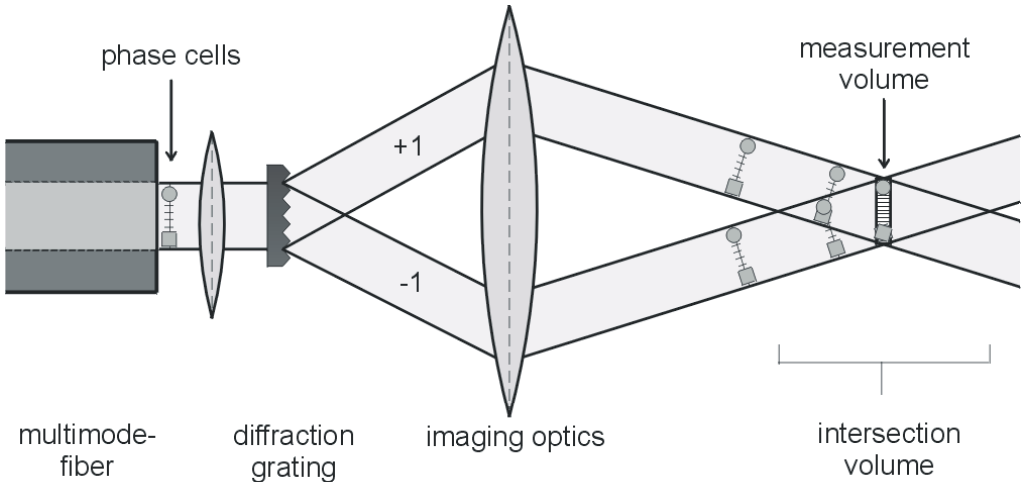

Figure 2: Limitation of the interference volume by the use of spatial low coherent light composed of uncorrelated phase cells.

The resulting effect on an LDA-system - which can be regarded as a Mach-Zehnder-interferometer – is shown in fig. (2). The light from a multimode-fibre is divided into two beams and reunited by imaging optics. Particles scatter light from the measurement volume that interfere at a detector. At the fibre endface the light can be regarded as an assembly composed of different phase cells, each of finite size – indicated in fig. (2) – and mutually uncorrelated among one another [10]. The mean size of these cells and therefore their mean distance is called coherence distance or transversal coherence length. Interference can only occur from light which descends from the same phase cell, each having ideal coherence properties. In each point of the intersection volume a certain cell of one beam overlaps with one cell of the

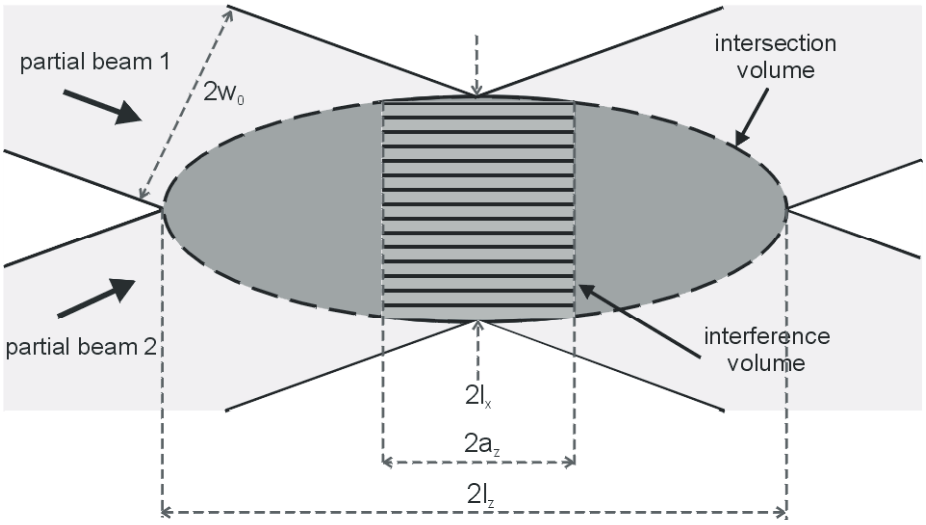

Figure 3: Intersection volume and interference volume of two crossing multimode laser beams. The lines indicate the $1/e^2$-bordes of the laser beams and the interference volume. The function of the visibility in the longitudinal direction is described by a Gaussian function, whereas in the lateral direction it is described by a rectangular function.

otherbeam. In the marginal regions only unequal phase cells overlap so that, because of their missing correlation, no interference occurs. In the centre region, equal phase cells coincide and an interference pattern develops.

Consequently, the intersection volume of the two laser beams and the measurement volume, i.e. the interference volume, are no longer identical. This circumstance is illustrated in figs. (2) and (3). Because of the low degree of spatial coherence the interference volume is restricted to a flat disc positioned in the middle of the beam intersection and perpendicular to the optical axis. Its elongation, i.e. its full length along the optical axis, is denoted as $2a_z$.
It turns out that by a change of LDA sending optics, the length of the interference volume $2a_z$ is exactly proportional to the length of the intersection volume $2l_z$. It is therefore practical to introduce a dimensionless factor

$$\xi := \frac{a_z}{l_z} \qquad \text{with} \quad l_z = \frac{w_0}{\sin\theta} \tag{2a, 2b}$$

($2w_0$: beam waist diameter, θ: crossing half angle) which in the following is referred to as the "reduction factor", denoting the ratio of the length of the interference volume (=measurement volume) to the length of the intersection volume. Combining eqs. (2a) and (2b) the entire effective length of the measurement volume can be expressed in terms of the beam-quality-dependent reduction factor ξ:

$$2a_z = \frac{2w_0}{\sin\theta} \cdot \xi(M^2) \tag{3}$$

The reduction factor ξ is equal to 1 for ideal spatial coherent light, e.g. light coming from a singlemode fibre. In any other case it is smaller. It changes if the coherence distance is altered, which can be achieved through a change of the fibre parameters and the wavelength, see eq. (1).
The dependence of the reduction factor from the beam quality factor was studied experimentally by combining two laserdiode arrays with different wavelengths, successively following with three multimode-fibres of the step index type so that six different M^2-values resulted. A LDA with a set-up as described in the following section was used to measure a_z and l_z in dependence of M^2. The results are plotted in fig. (4). The monotonous decline of the curve meets the expectations. From this it becomes evident that an increasing M^2-value lowers the degree of spatial coherence, i.e. the coherence distance, and therefore the length of the volume where interference can occur. Figure (4) shows also that the data points can be fitted in good approximation with a hyperbolic curve but an exact formula has not been derived yet. At M^2=350 a discrepancy between the fit curve and the data point occurs, indicating a systematic error during the measurement or an inappropriate fit function. The curve should of course have a fixed point at $\xi(M^2=1)= 1$, meaning that for the case of ideal spatial coherence (e.g. with light emitted from a single-mode fibre) the intersection volume of the two laser beams and the interference volume are identical and eq. (3) reduces to the known eq. (2b). The curve, which exhibits the best fitting to the measuring points, is given by $\xi(M^2)= 1.35/M^2$ and shows for $\xi(M^2=1)$ a slightly higher value than expected.

II. c) The speckle-effect

In contrast to a single mode fibre the cross section of a beam emitted from a multimode fibre shows local intensity fluctuations, which are known as speckles. The visibility of a speckle pattern $\eta_{Speckle}$ can be defined in the same way as the visibility of an interference pattern (see section II.b).
The mean size of the speckles depends on the number of guided modes [9]. Speckles are caused by interference from all coherent guided modes in the fibre. Different path lengths arise from the modes propagating with different angles to the core/cladding interface by total reflection. The maximum path length difference occurs between the lowest and the highest possible mode and is approximately given by [9]:

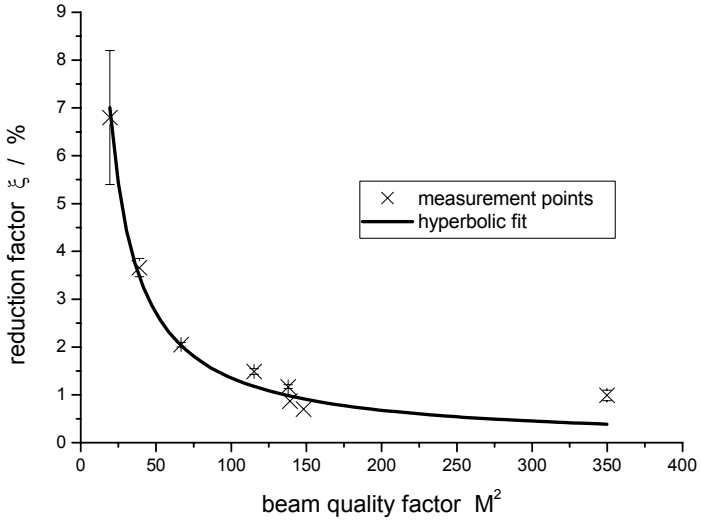

Figure 4: Dependence of the reduction factor ξ on the beam quality factor M^2.

$$L_D \approx \frac{1}{2} \cdot L \cdot A_N^2 \qquad (4)$$

where L denotes the length and A_N the numerical aperture of the fibre. This effect in multimode fibres is known as modal dispersion. In case of light with a high longitudinal coherence length $l_c=\lambda_0^2/\Delta\lambda$ (λ_0: centre wavelength, $\Delta\lambda$: width of the spectral line) the fibre output intensity profile is the result of a superposition of all guided modes under consideration of their relative phase relations. The speckle visibility is then, of course, very high. In the fibre only those modes will interfere whose path length differences are shorter than the coherence length. All other modes will add incoherently and thereby reduce the visibility of the speckle pattern. Speckles introduce an additional parasitic noise on the burst signal so that it is necessary to reduce the speckle visibility. From the preceding explanation, it follows that to this end, long fibres with high numerical apertures and light sources with short coherence lengths should be used.

In order to measure the visibility of the speckle pattern the light of a laser diode array (wavelength λ= 807 nm, coherence length $l_c\approx$ 513 µm) was coupled into three different fibres. The light emitted from the fibre endface was imaged with a Kepler telescope into free space in order to scan the beam profile. Small water droplets with diameters around 1.5 µm acted as point-like scattering objects. To collect the stray light, a receiving unit consisting of a single lens and a subsequent multimode fibre leading to an avalanche photo detector were placed tilted with respect to the optical axis and directed towards the beam waist. Viewing the detector time signal on an oscilloscope, the speckle visibility $\eta_{Speckle}$ was evaluated by $\eta_{Speckle}= (I_{Max}-I_{Min})/(I_{Max}+I_{Min})$, where I_{Max} und I_{Min} denote the maximum and minimum speckle intensities, respectivly. The estimated average speckle sizes were 2.8 µm and 1.2 µm for the A_N= 0.16 fibres and the A_N= 0.37, respectively.
The measured speckle visibilities are summarised in the following table (L: fiber length, L_D: calculated maximum modal dispersion, coherence length $l_c\approx$ 513 µm):

core-diameter/µm	A_N	L / m	L_D / mm	$\eta_{Speckle}$ / %
200	0.16	5	26	15.4
400	0.16	2	64	10.9
50	0.37	30	2053	5.6

Table 1: Results of the measurements of the speckle visibilities

As expected, the speckle visibility can be reduced by increasing the modal dispersion. The modulation by the speckles can now be neglected compared to that caused by the fringe system. For a detailed investigation of the speckle influence we refer to [11].

It is important to note, that a decrease of the longitudinal coherence length leads only to a reduction of the speckle visibility, but not to a reduction of the visibility of the fringe pattern. Though both effects arise from interference, they are not dependent on one another because the speckle interference takes place within *one* beam, i.e. the multimode fibre, whereas the fringe system in the centre of the intersection volume is caused by interference from *both* partial beams generated by beam-splitting. In fact, even at very short coherence lengths the fringe system will show complete modulation, as long as only the path length difference of the two partial beams is shorter than the coherence length,

which can easily be accomplished if a grating is used for beam-splitting. In contrast, due to the reasons mentioned above the visibility of the speckle pattern will decrease continually as the coherence length of the light source reduces. This gets evident from experiment: A burst signal taken with a set-up described in Chapter III with water droplets of approx. 3 µm diameter is shown in fig. (1). The Doppler modulation is clearly evident. Speckles can be recognised as small, non periodic oscillations on the signal. Since their modulation is significantly smaller than the modulation caused by the fringes, they can be neglected. In the frequency spectrum a sharp, clear peak occurs, so that a precise determination of the Doppler frequency is still possible. Another characteristic of the MMF-LDA can be seen here: Envelopes of the burst signals are rectangular, whereas in the case of LDA´s employing single mode radiation they are Gaussian. This is caused by the flat-top intensity profile of the multimode radiation. The fibre end face can be regarded as a homogenous shining object imaged through the optical system.

III. Experimental set-up and characterisation of the measurement volume

The experiments for the characterization and for the fluid flow measurements were carried out with an LDA-set-up mounted on an optical bench, see fig. (5). Light from a laser diode array (output power 700 mW at 810 nm) was launched by a lens system into a multimode fibre of step index type with 100 µm core diameter and 0.22 numerical aperture. The theoretical value of $M^2 \approx 43$ was confirmed by a beam quality measurement of the emitted radiation. For the effect of umode scrambling, the fibre was plaited through a row of bolts (bend radii ≈1 cm, power loss <1%). The fibre output light was imaged with a Kepler telescope consisting of achromatic lenses, onto a phase grating (grating constant 10 µm, design wavelength 800 nm) for beam splitting. A grating is employed since it fulfils the requirement for achromatic imaging which is needed for the two-wavelength homodyne-technique as described in the following section. Furthermore it is less sensitive with respect to alignment and independent upon the orientation of polarisation. A second Kepler telescope was used to collimate and intersect the partial beams. In the Fourier plane of the second telescope beam stops were placed to suppress the 0th, ±2nd and higher diffraction orders, so that only the +1st and -1st diffraction orders were used to form the measurement volume. 100 mW laser power was available in the measurement volume. The set-up was mounted on a motorized translation table. For the detection of the stray light a receiving unit was aligned towards the measurement volume. It consisted of a single lens collecting the stray light and launching it into a multimode-fibre, which was connected to an avalanche photo detector. Signals were processed by a PC with a 12-Bit analogue-digital-converter card. A LabVIEW program controlled the data acquisition, calculated a Fast-Fourier-Transformation (FFT) and switched the movement of the motor table.

For a characterization of the sensor the measurement volume was scanned with dust particles of a few micrometer size. They were located on a polished glass plate with an radius of (92079±7) µm which rotated with a constant velocity driven by a stepper motor [12]. The receiving optics was placed in a backward-scattering arrangement. During the scanning a PC recorded the height and frequency of the FFT-peak. Since the DC-part remained nearly constant, the height of the FFT-peak is a measure for the visibility of the fringe system. Results are plotted in Fig. (6): Fig. (6a)

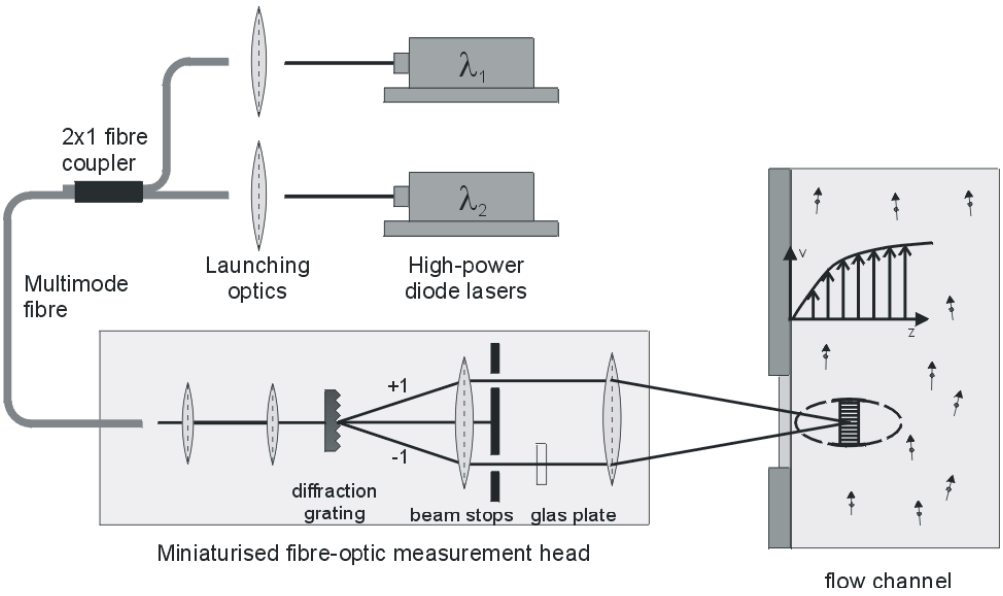

Figure 5: Experimental set-up of the multimode fibre laser Doppler anemometer. Two diode lasers with different wavelengths are needed to achieve directional discrimination by means of the homodyne technique.

shows the interference contrast normalized to unity along the optical axis. The curve can be fitted well with a Gaussian function. The full $1/e^2$-length is obtained to 80 µm determining the length of the measurement volume. A MV of 40 µm was recently demonstrated, see [11].
In the lateral direction the elongation was measured to 300 µm. With a fringe spacing of about 3 µm 100 fringes and therefore 100 signal periods occur, allowing a precise measurement of accelerated particle movements. It should be emphasized, that the long elongation of the measurement volume is now aligned in the direction of the velocity component which is to measure, i.e. the flow direction, whereas the short elongation lies perpendicular to the flow, where a high spatial resolution is needed. The orientation of the measurement volume of the MMF-LDA is rotated by 90° compared to conventional LDA employing single-mode radiation, see fig. (7).
Fig. (6) b) shows the fringe spacing inside the MV. A low variation of $4.8 \cdot 10^{-4}$ results and is therefore significantly smaller than that of commercial LDA´s. The MMF-LDA combines in one set-up the advantages of having either a high spatial resolution or low virtual turbulence. This is due to the multimode-radiation which shows a behaviour like classical geometrical light propagation with plane wavefronts.

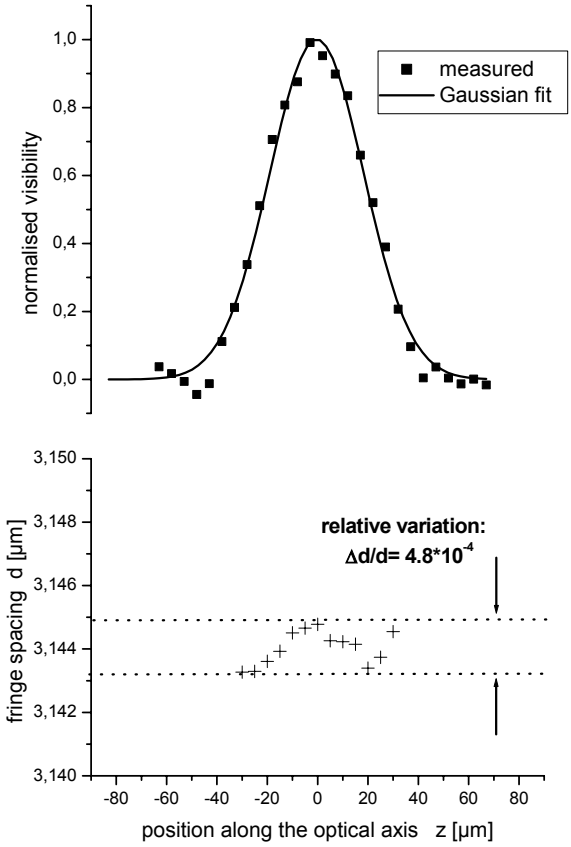

Figure 6: Characterisation of the measurement volume: a) interference contrast, b) fringe spacing.

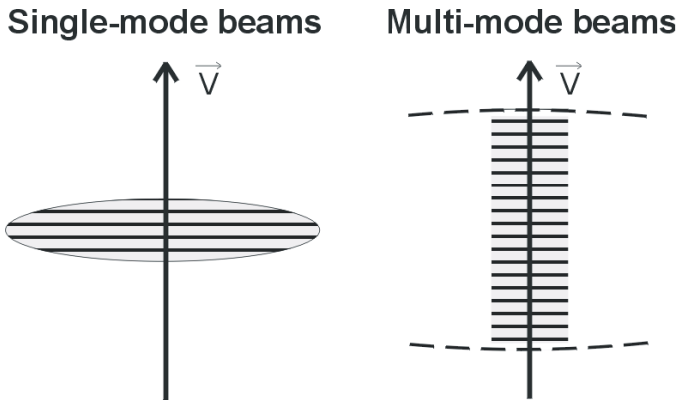

Figure 7: Schematic comparison between measurement volumes employing single-mode laser beams (left) and multimode laser beams at the sending optics.

IV. Directional discrimination using the two-wavelength homodyne-technique

To achieve directional discrimination of the passing particle the MMF-LDA can be extended by means of the two-wavelength homodyne-technique [13], see fig. (5). With this method a passive, miniaturised measurement head can be realised. No active frequency shift elements, which are bulky and sensitive to electro-magnetical disturbances, are needed. With the homodyne-technique, a bi-chromatic radiation is employed, so that two measurement volumes with similar properties are generated. A shift of the fringes of a quarter of the spacing corresponding to a phase shift of $\pi/2$ can be achieved. Particles passing the common measurement volume now scatter a bi-chromatic stray light which, after wavelength sensitive detection, forms sine/cosine signal pairs. The directional discrimination is attained by phase evaluation of the burst signals of each wavelength. For the function of the homodyne-technique a constant phase shift within the entire measurement volume is required. A prerequisite is a constant and identical fringe spacing for both fringe systems. This prerequisite is fulfilled by the employment of a diffraction grating for beam splitting which

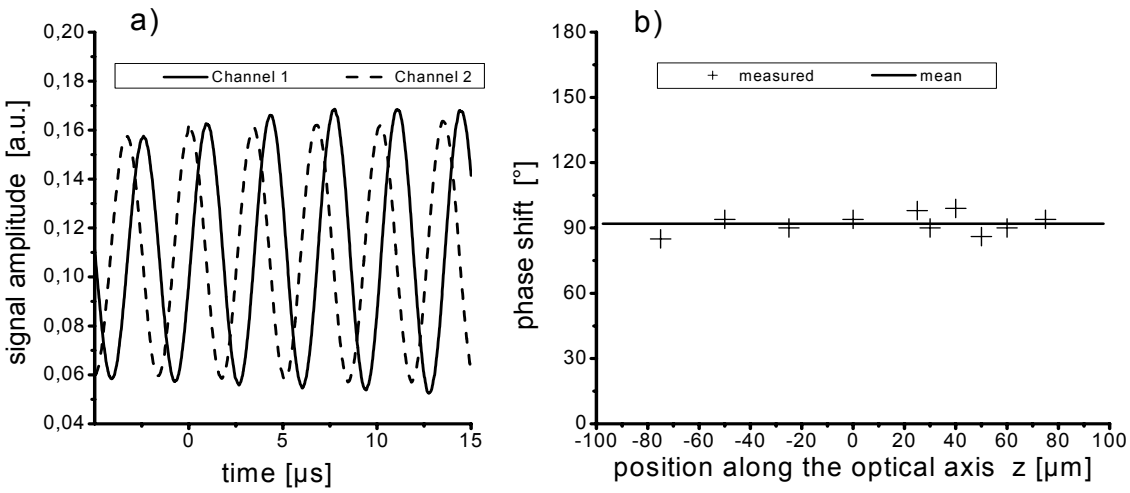

Figure 8: Directional discrimination using a homodyne MMF-LDA: a) sine/cosine signal pairs are generated by bi-chromatic radiation. b) A constant phase shift of 90° can be generated within the entire measurement volume.

provides achromatic fringe systems, while the geometrical light propagation of the multimode radiation ensures an adequate constant fringe spacing, see fig. (6b).
To verify the function the radiation of two different laser diode arrays (λ_1: 810 nm, λ_1: 660 nm) were combined by means of a 2x1 fibre coupler, see fig. (5), and a measurement volume of length 200 µm was created. In order to shift the fringes systems against each other, a glass plate was introduced into one partial beam in the Fourier plane of the last Kepler telescope. Since the dispersion is different for both wavelengths, different retardations result and therefore a relative shift of the fringe systems. Fine adjustment to a phase shift of $\pi/2$ was achieved by tilting the glass plate a few degrees, thus changing the effective optical path through the plate.
The bi-chromatic measurement volume was scanned with a wire of 4 µm diameter mounted on an optical chopper, which rotated with constant velocity. The bi-chromatic stray light was separated with a dichroic mirror and then led onto avalanche photodetectors. Fig (8) indicate the results: Fig. (8a) shows burst signal pair with $\pi/2$ phase shift. Within the measurement volume it is constant along the optical axis, fig. (8b). Therefore, the MMF-LDA meets the requirements of the homodyne technique for directional discrimination.

V. Wind tunnel measurements of flat-plate boundary layers

The function of the multimode-fibre LDA as described in section III was verified in a closed-loop wind tunnel of the Göttingen type with an open test section. DEHS (diethylhexyl sebacate) droplets of 2.5 µm mean diameter acted as scattering objects. At the fluid flow measurements a validation procedure has been used in the PC measurement program in order to distinguish between particles flying through the measurement volume and those flying through the marginal regions of the intersection volume, where no interference fringes occur. Burst signals were only taken into account if their FFT-peak height exceeded a certain threshold.
The wind tunnel was known from hot-wire measurements to have a degree of turbulence lower than 0.4% [14]. Prior to the boundary layer measurements, the free stream of the wind tunnel was investigated with respect to its turbulence properties. Approx. $1.1 \cdot 10^4$ burst signals were evaluated. Fig. (9) shows the probability density function. The mean velocity and the degree of turbulence result to:

$$v_\infty = (8.176 \pm 0.025)\ \text{m/s}\ , \qquad Tu_{\text{wind tunnel}} = \frac{\Delta v_\infty}{v_\infty} = 0.30\ \%$$

As remarked in the introduction, such a low degree of turbulence can conventionally only be measured with a large measurement volume ensuring a low variation of fringe spacing (virtual turbulence). Here the MMF-LDA overcomes this drawback by combining a high spatial resolution *and* a low virtual turbulence.
The present measurement was also used to determine higher order moments, the skewness factor S and flatness factor F, which are defined by $S = \langle v'^3 \rangle / \langle v'^2 \rangle^{3/2}$ and $F = \langle v'^4 \rangle / \langle v'^2 \rangle^2$, where $\langle v'^n \rangle$ is the n-th order moment. They describe the shape of the probability density function of the measured velocity values. In the case of homogenous isotropic turbulence the higher order moments attain the values S=0 and F=3, which are valid for a Gaussian distribution [15]. The experimental results were S= -0.20 and F= 3.40 and are in a good agreement with the values for the expected Gaussian distribution. In turbulent boundary layers the skewness and flatness factor differ notably from these values [15].

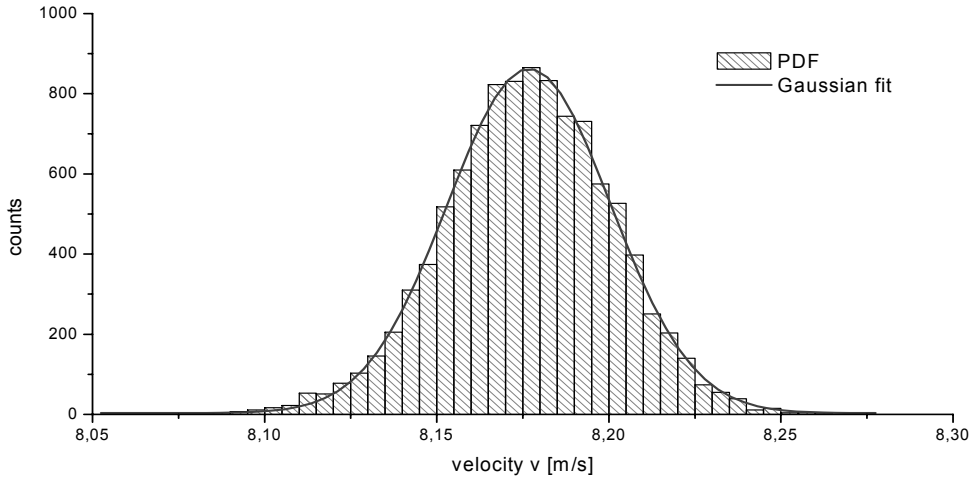

Figure 9: Probability density function for turbulence analysis of the free wind tunnel stream.

For the measurements of the Blasius boundary layer, a glass plate was placed in the centre of the test section. The MMF-LDA was mounted on a motorized translation table in order to scan the velocity profile perpendicular to the plate. The receiving optics were placed in a forward scattering arrangement but approx. 20° inclined with respect to the plane of the partial beams so that reflexes of the glass plate had only a smaller influence. The optical power of 100 mW in the measurement volume was sufficient to produce burst signals from the avalanche photodetectors large enough for acquisition with a PC analogue-digital converter card. A LabView program controlled the table movement and the signal processing. At each z-position, 20 valid burst signals were taken.

Velocity profiles were taken at different positions, x, behind the leading edge of the glass plate and for different free stream velocities v_∞. Fig. (10) shows the boundary layers for Reynolds numbers $Re_x = 5.8 \cdot 10^3$, $2.3 \cdot 10^4$, $5.8 \cdot 10^4$, where Re_x is represented by xv_∞/ν, with $\nu = 1.5 \cdot 10^{-5}$ m^2/s as the kinematic viscosity of air. Since the Reynolds numbers are significantly smaller than $3.5 \cdot 10^5 \ldots 1 \cdot 10^6$, which is considered as the critical range for laminar to turbulent transition, laminar boundary layers were available. In order to compare the measured boundary layers with Blasius´ theory, normalised co-ordinates (v/v_∞ and $\eta = z\{v_\infty/(2\nu x)\}^{1/2}$) have been used. The theoretical solution $f' = f'(\eta)$ was gained by solving the Blasius equation $f''' + f \cdot f'' = 0$ (dash means differentiation by η) with the initial conditions $f(0)=0$, $f'(0)=0$ and $f''(0)=0.4696$ [16] with the mathematics program Maple. This solution has also been added to the plot, indicating the good agreement between theory and experiment.

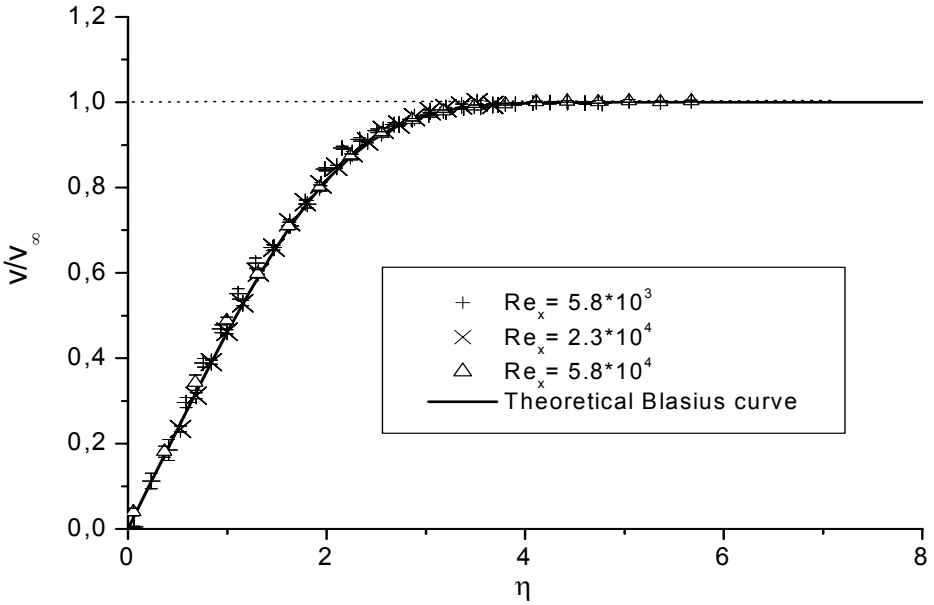

Figure 10: Measured velocity profiles of boundary layer flows for different Reynolds numbers in normalised co-ordinates v/v_∞ and $\eta = z\,(v_\infty/(2\nu x))^{1/2}$. A good agreement with the theoretical Blasius boundary layer occurs.

For boundary layer measurements, special interest lies on the wall shear stress τ, since it determines directly the skin friction drag of aerodynamic devices.
With $\mu = 1.8 \cdot 10^{-6}$ Ns/m^2 as the kinematic viscosity of air the wall shear stress is defined as:

$$\tau = \mu \left. \frac{d\mathrm{v}}{d\mathrm{z}} \right|_{z=0}$$

if the object is located at z=0. From the measured profiles the wall shear stress τ was evaluated from the slope of a linear regression in the ascending part of the curves. For a fixed position x= 51 mm behind the leading edge and variied free stream velocity v_∞ results are plotted in fig. (11). For a comparison, the theoretical function was also calculated: The local wall shear stress for a laminar boundary layer is $\tau = 0.332\mu(v_\infty^3/(\nu x))^{1/2}$, [16]. This function was also added to the plot and indicates again the good agreement between experiment and theory. Consequently, the presented sensor is well suited for measurements of shear flows.

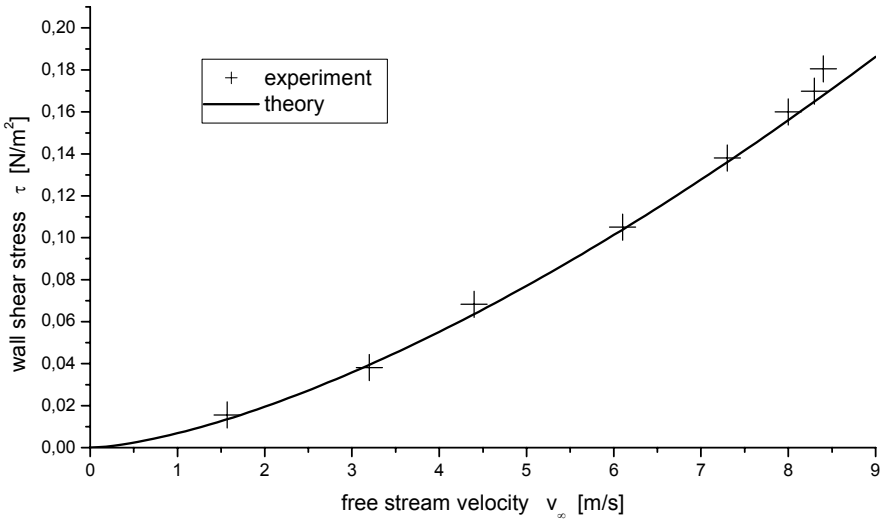

Figure 11: Wall shear stress τ measured 51 mm behind the leading edge of the glass plate for different free stream velocities v_∞.

VI. Conclusion

In this contribution the employment of multimode fibres for beam delivery in laser-Doppler-anemometers was presented.
The advantages of the mulitmode-fibre laser-Doppler-anemometers (MMF-LDA) can be summarised as follows:

- High-power and low-cost diode lasers can be employed
- Only low alignment effort is needed for coupling into multimode-fibres.
- Short measurement volumes for high spatial resolution can be generated due to the low degree of spatial coherence
- A low variation of fringe spacing, i.e. "virtual turbulence"
- Directional discrimination can be attained by homodyne technique without using active frequency shift elements.

It was demonstrated that due to the low degree of spatial coherence of the multimode-radiation, the length of the measurement volume can be reduced drastically with regard to the length of the intersection volume.
The presented principle is due to small measurement volume lengths capable of measuring velocity gradients with high spatial resolution. The length of the measurement volume decreases relative to the length of the intersection volume with the beam quality, characterised by the beam quality factor M^2. An M^2-value of 150 leads to a measurement volume having only $\approx$1% of the length of the intersection volume.
It turns out that the variation of the fringe spacing within the measurement volume cannot be described with the Gaussian-beam model, which is adequate in single-mode beams. Due to the flat top intensity profile the burst signals of particles passing through the measurement volume show rectangular envelopes.
It was demonstrated how the disturbing speckle effect, as it arises from multimode fibres, can be reduced below visibilities of 6%. The remaining speckle visibility can be neglected so that a precise Doppler frequency estimation is still possible. It was shown that the speckle effect and the interference fringe system are affected independently from each other, so that a fringe system with full modulation but with a low speckle visibility can be accomplished.
Directional discrimination can be attained using the two-wavelength homodyne-technique. It was shown that a bi-chromatic measurement volume can be realised with a constant fringe spacing shift of $\pi/2$. Passing particles generate sine/cosine burst signal pairs, whose phase shift contain information about the direction.
Fluid flow measurements were carried out with a measurement volume of 80 µm length, 100 mW available laser power, 100 fringes and fringe spacing variation of $5 \cdot 10^{-4}$. Blasius boundary layers at a glass plate as well as wall shear stress were measured and compared with theory. An excellent agreement confirms the function of the sensor.
As a result, a powerful, easy to adjust laser Doppler anemometer can be accomplished by the employment of high-power, low-cost diode lasers and multimode-fibres. The multimode-fibre laser Doppler anemometer (MMF-LDA) combines the advantages of both a short measurement volume of a few ten µm guaranteeing a high spatial resolution as well as low virtual turbulence of less than 0.1% in one device. It is therefore well suited for the measurement of shear flows.

Acknowledgements

The authors would like to thank T. Razik for developing the LabVIEW-programs, M. Boivin for his professional work with the experiments, A. Isemann for the assignment of the Polaroid laser-diode array and Dr. P. Regenfuß and D. Leong for proof-reading this paper.
Thanks are due to Dr. H. Müller (PTB/Braunschweig) for making possible the LDA calibration.
The support from E.-S. Zanoun, Dr. S. Becker, H. Lienhart and Prof. Dr. F. Durst, all LSTM/Erlangen, for making available the wind tunnel is greatly acknowledged.
This work was funded by the Deutsche Forschungsgemeinschaft (DFG, FKz: Cz 55/4-4).

References

[1] E.-J. Nijhof, W.S.J. Uijttewaal, R.M. Heethaar, “Blood particle distributions accessed by microscopic laser-Doppler velocimetry”, SPIE Vol. 2052 p. 675, Laser Anemometry Advances and Applications, p.187, 1993

[2] P. Miles, P. Witze, "Evaluation of the Gaussian beam model for prediction of LDV fringe fields", 8th International Symposium on Applications of laser techniques to fluid mechanics, paper 40.1, Lisbon/Portugal 1996

[3] S.L. Kaufmann, L.M. Fingerson, “Fiber Optics in LDV Applications”, on the International Conference on Laser Anemometry – Advances and Applications, 16th –18th Dec. 1985, Manchester/UK

[4] B. Ruck, F. Durst, “Laser-Doppler-Anemometer auf der Basis von Gradientenfasern”, Heft 6, pp. 243-249, Technisches Messen 1983

[5] S. Bopp, C. Tropea, L. Zhan, “The use of graded-index fibers in fiber-optic laser-Doppler anemometry probes”, Rev. Sci. Instrum. 60(10), Oct. 1989

[6] M. Haag, M. Brandner, "Diode lasers - an innovative tool for production", p. 36, LaserOpto 03/2000

[7] D.P. Hand, J.D. Entwistle, R.R.J. Maler, A. Kuhn, C. A. Greated, J.D.C. Jones, “Fibre optic beam delivery system for high peak power laser PIV illumination”, Meas. Sci. Technol, Vol. 10, pp. 239-245, 1999

[8] D. Su, A.A.P. Boechat, J.D.C. Jones, “Beam delivery by large-core fibers: effect of launching conditions on near-field output profile”, Applied Optics, Vol. 31, No. 27, p. 5816, 1992

[9] R.D. Morgan, D.J. Anderson, J.D.C. Jones, W. Easson, C. Greated, “Design of fibre optic beam delivery system fo r particle image velocimetry”, SPIE Vol. 2052 p. 675, Laser Anemometry Advances and Applications 1993

[10] N. Takai, T. Asakura, “Statistical properties of laser speckles produced under illumination from a multimode optical fibre”, J. Opt. Soc. Am. A, Vol.2, No.8, p.1282, Aug. 1985

[11] L. Buettner and J. Czarske, “A multimode-fibre laser-Doppler anemometer for highly spatially resolved velocity measurements using low-coherence light”, Meas. Sci. Technol. 12, pp. 1891-1903, 2001

[12] H. Mueller, R. Kramer, V. Strunck, B. Mickan, D. Dopheide, “Laser-Doppler-Anemometer zur Darstellung und Weitergabe der Einheit Strömungsgeschwindigkeit”, 9th conference “Lasermethoden in der Strömungsmeßtechnik”, pp. 24.1-24.8, Winterthur/Switzerland, 18.-20.09.2001

[13] L. Buettner, J. Czarske, C. Fallnich, "Diodengepumpte Faserlaser in achromatischen LDA-Systemen mit Richtungserkennung und Mehrpunktmessung", 8th conference "Lasermethoden in der Strömungsmeßtechnik", paper 8, Munich/Germany 2000

[14] F. Durst, E.-S. Zanoun, M. Pashtrapanska, “In situ calibration of hot wires close to highly heat-conducting walls”, Experiments in Fluids Vol. 31, pp. 103-110, 2001

[15] M. Fischer, J. Jovanovic and F. Durst, “Reynolds number effects in the near-wall region of turbulent channel flows”, Physics of Fluids Vol. 13, No. 6, pp. 1755-1767, June 2001

[16] H. Schlichting, „Boundary layer theory“, McGraw-Hill, New York/USA 1987